P1.17

TEMPORAL SAMPLING ERRORS IN ATMOSPHERIC AND SURFACE FLUXES

Martial P. A. Haeffelin*, Takmeng Wong+ and David F. Young+

*Virginia Polytechnic Institute and State University
Blacksburg, VA 24061-0238
+NASA/Langley Research Center
Hampton, VA 23681

1. INTRODUCTION

The Cloud and the Earth's Radiant Energy System (CERES) is a NASA space-borne measurement program for monitoring the radiation environment of the Earth-atmosphere system (Wielicki et. al., 1996). The first CERES instrument is scheduled to be launched in November 1997. In addition to top-of-atmosphere (TOA) fluxes, CERES will also be producing atmospheric and surface flux data based on TOA-flux-constrained radiative transfer calculations. The satellites that carry the CERES instrument do not provide continuous temporal coverage of the Earth surface. The retrieval of atmospheric and surface fluxes using TOA observations as constraints to the radiative transfer model inherently contains the same temporal aliasing problem. If uncorrected, this aliasing effect can introduce significant temporal errors into the computed climatology of these fluxes. In Sec. 2. of this paper we explore the possible magnitude of this temporal sampling problem using a set of high quality and high temporal resolution data. Techniques for correcting this sampling bias and their results are given in Sec. 3. Conclusions and future work are presented in Sec. 4.

2. DATA ANALYSIS

Time interpolation procedures for broadband LW and SW fluxes at the TOA have been developed for the Earth Radiation Budget Experiment to estimate diurnal cycles, daily- and monthly-mean fluxes based on a limited number of satellite observations (Brooks et. al., 1986). Several studies (Stowe, 1987; Standfuss et. al., 1993; Wielicki et. al., 1995) showed that restricted time sampling is the main source of error in estimated monthly-mean TOA quantities. In the SW domain, for example, the mean diurnal range over ocean and land regions is about 2.5 times greater in the presence of clouds than in clear-sky conditions. Uncertainties arise when significant variations occur over time periods shorter than the sampling time step.

It can be expected that time sampling will also be a significant source of error in the determination of atmospheric and surface fluxes. As part of the CERES data products vertical profiles of fluxes in the atmosphere and at the surface will be estimated at synoptic times, i.e. every three hours UTC. Daily and monthly-mean radiative fluxes can be computed directly by averaging the synoptic fluxes. This approach is expected to introduce biases in the mean fluxes which can be related to the sampling patterns and the actual diurnal cycles of both incoming solar radiation (SW domain) and cloud cover activity (LW and SW). In order to estimate possible uncertainties in the current processing techniques, a high quality and high temporal resolution dataset is used to simulate conditions of sparse time sampling. This dataset, the simulation techniques and their results are given below.

2.1. The CAGEX Dataset

The CERES/ARM/GEWEX Experiment (CAGEX) dataset, developed from the intensive observation period over the ARM CART* site in Oklahoma, USA, in April 1994, is used in our analysis. The site is defined as a 3x3 .3-degree spatial grid centered at 36.61°N latitude, and 97.49°W longitude. This data base consists of atmospheric soundings, aerosol and cloud properties retrieved from satellite as well as cloud data and radiative fluxes based on surface measurements. In addition, vertical atmospheric profiles of shortwave and longwave radiative fluxes are computed from the surface to the TOA

*Corresponding author address: Dr. Martial P. A. Haeffelin, NASA/Langley Research Center, MS 420, Hampton, VA 23681-0001, Tel: 1 (757) 864-9590, Fax: 1 (757) 864-7996, Email: m.p.haeffelin@larc.nasa.gov

*Clouds and Radiation Testbed (CART) site of the Atmospheric Radiation Measurement (ARM) program.

using a radiative transfer model (Charlock and Alberta, 1996).

The data are available with a half-hourly temporal resolution from 1409 GMT to 2239 GMT (18 daytime measurements per day) over a 26-day period. The vertical resolution of soundings and flux profiles is about 25 mbar with slightly higher resolution between the surface and 700 mbar as well as above 100 mbar for a total of 48 levels.

2.2. Data Analysis Technique

As the base line and truth set for our analysis, daytime SW and LW daily-mean vertical profiles of fluxes, $\bar{F}$, are computed based on the 18 half-hourly estimates F_j of the dataset as

$$\bar{F} = \frac{1}{18} \sum_{j=1}^{18} F_j \ . \tag{1}$$

To estimate the possible magnitude of the temporal sampling problem in CERES data processing we perform simulation studies using 3-hourly sampling patterns of LW and SW atmospheric and surface flux data. Three samples are obtained by sampling the 18 half-hourly estimates every three hours. Cloud information retrieved from geostationary satellite observations are typically available at 00, 03, 06, 09, 12, 15, 18 and 21 GMT. Therefore we choose to use the observations corresponding to 1509, 1809 and 2109 GMT as samples for our error analysis which corresponds to 0909, 1209 and 1509 LST.

Using the sampled data, the daytime LW and SW daily-mean vertical profiles of fluxes, $\bar{F}_{spl}$, are computed based on the N sampled estimates F_n of the dataset as

$$\bar{F}_{spl} = \frac{1}{N} \sum_{n=1}^{N} F_n \ . \tag{2}$$

Standard error analyses, including mean, standard deviation and root mean square (rms) errors are then performed for all-sky and clear-sky datasets to determine the magnitude of the sampling error. For a particular simulated dataset, the sampling error is defined as

$$\epsilon_{spl} = \bar{F} - \bar{F}_{spl} \ , \tag{3}$$

where a positive error indicates an underestimation and a negative error suggests an overestimation. Days with missing data are left out of the analysis to prevent any bias related to the number of samples. Results for all-sky and clear-sky conditions are discussed below.

2.3. Results

2.3.1. All-Sky Data

Table 1 shows the all-sky results in terms of the bias and rms error between the truth and simulated mean fluxes. Results are based on the data of the central pixel for 19 fully sampled days. Bias and rms errors are computed over all 48 atmospheric levels. The largest biases and rms errors are found for SW fluxes while small errors occur in the LW components. As expected, the monthly rms error is significantly less than the daily-mean rms error due to compensation between under- and overestimations related to sampling. In the SW domain bias can be attributed to two effects: (1) the three samples do not cover the entire diurnal range which, with the present sampling pattern provides an overestimation of the monthly mean; (2) due to diurnal variations in cloud cover, the three samples may not be representative of the average diurnal variations of the flux. In the LW domain the latter effect dominates the bias.

Table 1: Differences between fluxes (daily- and monthly-mean in W/m^2) computed from 1/2-hour and 3-hour sampled data.

(W/m^2)	Mean Flux	Bias	RMS	
			Daily	Monthly
LW UP	300	1.0	6.8	1.2
LW DN	145	-0.6	7.6	1.6
SW UP	275	-10.5	29.0	12.4
SW DN	750	-14.8	36.8	16.9

Fig. 1 shows the vertical profiles of the difference between monthly-mean fluxes computed from the original dataset and that computed from sampled data. In the SW domain biases in the cloud-free portion of the atmosphere are significant and remain constant from 200 mbar to the TOA. Cloud layers are found at different levels every day, between 800 and 200 mbar. In this vertical range the bias can be very large (>10 % in the case of upward SW flux). The vertical variability reveals the dramatic impact of clouds on the SW flux at any given atmospheric level. As expected, in the LW domain, biases are less sensitive to the presence of clouds. However, note that the vertical variability is somewhat larger between 800 and 200 mbar than above 200 mbar.

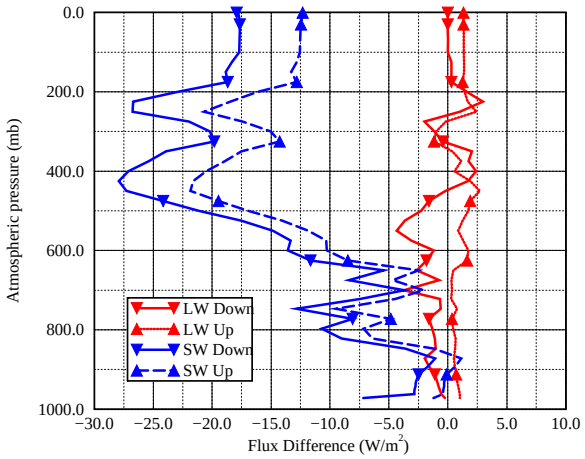

Figure 1: Vertical profiles of the difference between monthly-mean fluxes computed from 1/2-hour and 3-hour sampled data.

2.3.2. Clear-Sky Data

A similar analysis is performed on clear-sky days. We compute daily-mean fluxes for each component at all levels of the atmosphere using two different sampling patterns, 14-17-20 GMT and 15-18-21 GMT. In the former, the first sample is taken at 0809 LST while the last sample is at 1409 which produces an underestimated daily mean in the SW domain. In the latter, the samples are closer to and more centered around noon and produce an overestimated daily mean.

Table 2: Differences between daily-mean clear-sky fluxes (16 April 1994) computed from 1/2-hour and 3-hour sampled data.

	14-17-20 GMT		15-18-21 GMT	
(W/m^2)	Bias	RMS	Bias	RMS
LW UP	5.6	5.9	1.1	1.2
LW DN	0.8	1.8	0.2	0.4
SW UP	5.6	5.6	-3.4	3.4
SW DN	29.7	29.7	-17.1	17.1

Results are shown in Table 2 in a fashion similar to Table 1. Average upward and downward LW clear-sky fluxes computed from the truth set are 330 and 110 W/m^2, respectively. Average SW fluxes are 200 and 890 W/m^2. Errors in daily-mean (and in monthly-mean) fluxes are very sensitive to the sampling times. Note that all the rms error is due to the sampling bias. In the next section we show how these sampling errors can be reduced.

3. INTERPOLATION MODELS AND RESULTS

In order to reduce the temporal sampling error we developed high order temporal interpolation techniques. These models and their results for all-sky and clear-sky conditions are outlined below.

3.1. Linear Interpolation Models

Significant improvements to the computed fluxes can be obtained with a simple first-order linear interpolation model. Specifically, the bias can be reduced by interpolating between sampled values and extrapolating outside of the sampled ranged. In the SW domain this model is applied between two successive sampled fluxes F_i^{sw}/μ_i and F_{i+1}^{sw}/μ_{i+1} normalized by the cosine of solar zenith angle (CSZA) μ. The SW flux (both upward and downward) at any time t between the two sampling times is computed as

$$F^{sw}(t) = (at + b)\mu(t) \quad t_i < t < t_{i+1} \,, \qquad (4)$$

where the coefficients a and b are derived from the two sampled fluxes. The fluxes are extrapolated from the first sampling time to the first time step of the day (and from the last sampling time to the last time step of the day) by assuming that the first (last) sampled flux normalized by its CSZA remains constant over the extrapolation domain. For morning extrapolation this yields

$$F^{sw}(t) = F^{sw}(1)\frac{\mu(t)}{\mu(t_1)} \quad t_1 < t \,. \qquad (5)$$

In the LW domain the linear interpolation scheme is applied between two successive fluxes F_i^{lw} and F_{i+1}^{lw}. Extrapolation is not performed since for CERES data LW fluxes will be available on a 24-hour basis. The means are computed on the time range comprised between the first and last sampling times. The results of this model for both all-sky and clear-sky cases are shown below for simulated dataset with the 15-18-21 GMT sampling pattern.

3.1.1. All-Sky Data

Table 3 shows the all-sky results in terms of bias and rms errors for instantaneous, daily- and monthly-mean values. Compared to Table 1, the biases of the SW flux components are significantly reduced. The main advantage of the interpolation/extrapolation scheme is that the magnitude of the integrated daily flux is based on a full range of fluxes rather than just three flux samples. However

the extrapolation scheme will tend to underestimate fluxes for layers which are below the cloud top since we assume the SW flux follows the decreasing CSZA. Indeed, the CSZA dependence applies mostly to the direct component of the SW flux and is not as appropriate a model for the diffuse component. Reductions in rms errors are mainly due to the decreased bias.

Table 3: Differences between fluxes (daily- and monthly-mean in W/m^2) computed from 1/2-hour and 3-hour interpolated data.

(W/m^2)	Bias	RMS		
		Instant.	Daily	Monthly
LW UP	-0.7	13.9	5.3	1.2
LW DN	0.7	15.9	7.3	1.8
SW UP	-5.3	68.2	26.2	7.3
SW DN	-1.2	86.0	32.6	5.7

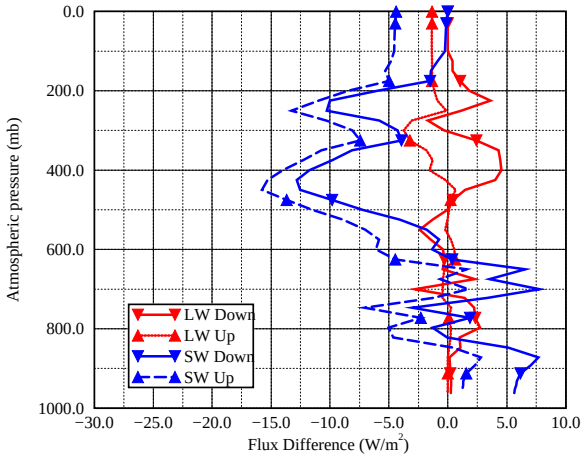

Figure 2: Vertical profiles of the difference between monthly-mean fluxes computed from 1/2-hour and 3-hour interpolated data.

Fig. 2 shows the vertical profiles of the difference between monthly-mean fluxes computed from the original dataset and that computed from sampled and interpolated data. Compared to Fig. 1 the bias for SW fluxes above the cloud top and below the cloud bottom is reduced to ± 5 W/m^2. However, the large vertical variations found within the cloud layer remain. They are mainly due to the diurnal variations of presence or absence of cloud at each atmospheric level. Hence interpolations are applied between two possibly different regimes and extrapolations can be in great error if the first (or last) sample is not representative of the cloudiness conditions in the extrapolation domain.

3.1.2. Clear-Sky Data

Table 4 shows the clear-sky bias and rms errors based on linear interpolation model. Compared to Table 2 the bias is considerably reduced and is less dependent on sampling time. The LW errors are essentially zero while some SW errors remain. In the SW domain the instantaneous rms error represents how well the CSZA variations account for the diurnal variations of the SW flux. The rms errors increase from essentially zero at the TOA to more than 15 W/m^2 at the surface. Maximum instantaneous SW errors can reach 50 W/m^2. In the LW domain the bias and rms errors are computed on the time range comprised between the first and last sampling times.

Table 4: Differences between instantaneous clear-sky fluxes (16 April 1994) computed from 1/2-hour and 3-hour interpolated data.

(W/m^2)	14-17-20 GMT		15-18-21 GMT	
	Bias	RMS	Bias	RMS
LW UP	0.0	0.1	-0.0	0.1
LW DN	0.0	0.0	0.0	0.0
SW UP	0.3	4.9	0.3	4.1
SW DN	-0.6	8.9	-0.6	7.1

In order to improve the SW instantaneous rms errors a higher order technique is developed.

3.2. Improved SW Clear-Sky Interpolation Scheme

In clear-sky conditions, diurnal variations of SW fluxes can be modeled very accurately by accounting for the CSZA dependence of the transmittance. The downward transmittance at any pressure level m in the atmosphere can be defined as

$$T_m^{\downarrow} = \frac{F_m^{\downarrow}}{F_{toa}^{\downarrow}} , \qquad (6)$$

where $F_m^{\downarrow}$ and $F_{toa}^{\downarrow}$ are the downward SW fluxes at level m and TOA respectively. The CSZA dependence of the transmittance can be modeled as

$$T_m^{\downarrow}(t) = A_m \exp[-B_m/\mu(t)] , \qquad (7)$$

where A_m can be thought of as the direct-to-total SW flux ratio and B_m represents a broadband SW

atmospheric optical thickness. Given two sampled fluxes at times t_1 and t_2, coefficients A_m and B_m can be determined from $T_m^{\downarrow}(t_1)$, $T_m^{\downarrow}(t_2)$ and Eq. 7. The downward SW flux at time t between the two sample times can then be computed as

$$F_m^{\downarrow}(t) = E_0(d)\mu(t)A_m \exp[-B_m/\mu(t)] \quad t_1 < t < t_2 \ , \tag{8}$$

where $E_0(d)$ is the solar constant for julian day d.

The upward SW flux can be expressed as

$$F_m^{\uparrow}(\mu) = a_m(\mu)F_m^{\downarrow}(\mu) \ , \tag{9}$$

where $a_m(\mu)$ is the albedo at pressure level m and for CSZA μ. By introducing the upward SW flux at the TOA and using Eq. 8, Eq. 9 can be rewritten as

$$F_m^{\uparrow}(\mu) = \frac{a_m(\mu)}{a_{toa}(\mu)} F_{toa}^{\uparrow}(\mu)A_m \exp[-B_m/\mu] \ . \tag{10}$$

The CSZA dependence of the albedo ratio a_m/a_{toa} can be modeled with an expression similar to that of the transmittance (Eq. 7). The CSZA dependence of the upward flux at the TOA can be represented by a directional angular model similar to those developed for ERBE (Suttles et. al., 1988).

We apply this detailed model to sampled clear-sky SW fluxes and compare the instantaneous interpolated values to the original CAGEX fluxes. Table 5 shows the bias and rms errors for 16 April 1994. Results for other clear-sky days in April 1994 are comparable. The instantaneous rms errors are significantly reduced compared to the linear scheme presented earlier. Maximum differences are now about 5 W/m^2 and vertically integrated rms errors are on the order of 1 W/m^2.

Table 5: Differences between instantaneous clear-sky fluxes (16 April 1994) computed from 1/2-hour and 3-hour interpolated (based on CSZA-dependence models) data.

	14-17-20 GMT		15-18-21 GMT	
	Bias	RMS	Bias	RMS
SW UP	-0.9	1.6	0.4	1.2
SW DN	-0.3	0.9	0.3	0.8

4. SUMMARY

CERES will be producing atmospheric and surface flux data based on TOA-flux-constrained radiative transfer calculations at synoptic times. Interpolation schemes are developed to provide improved daily- and monthly-mean fluxes computed from synoptic fluxes. We show that diurnal variations in both downward and upward clear-sky SW fluxes can be modeled accurately. The interpolated fluxes are in very good agreement with our truth set. In cloudy-sky conditions variability between sampling time cannot be modeled and random errors will always remain. However, bias in daily and monthly averages can be reduced by using available cloud information, which is the topic of a future study.

Acknowledgments: This work was supported by the NASA Langley Research Center under Grant # NCC 1 243. The authors would like to thank Tom Charlock and Tim Alberta for helpful advice concerning the CAGEX dataset.

REFERENCES

Brooks, D. R., E. F. Harrison, R. S. Kandel, P. Minnis, and J. T. Suttles, 1986: Development of algorithms of understanding the temporal and spatial variability of the Earth's balance. *Rev. of Geoph.,* **27,** 422–438.

Charlock, T. P., and T. L. Alberta, 1996: The CERES/ARM/GEWEX Experiment (CAGEX) for the retrieval of radiative fluxes with satellite data. *Bull. Amer. Meteor. Soc.,* **77,** 2673-2683.

L. L. Stowe, 1987: Earth radiation budget requirements review. NESDIS 41, NOAA.

Standfuss, C., H.-D. Hollweg and H. Graßl, 1993: The impact of an Earth radiation budget scanner aboard METEOSAT second generation on the accuracy of regional radiation budget parameters. *Meteorologisches Institut der Universität Hamburg,* **125144.**

Suttles, J. T., R. N. Green, P. Minnis, G. L. Smith, W. F. Staylor, B. A. Wielicki, I. J. Walker, D. F. Young, V. R. Taylor, and L. L. Stowe, 1988: Angular radiation models for Earth-atmosphere system. Reference publication 1184, NASA. Volume I - Shortwave radiation.

Wielicki, B. A., R. D. Cess, M. D. King, D. A. Randall, and E. F. Harrison, 1995: Mission to Planet Earth: role of clouds and radiation in climate. *Bull. Amer. Meteor. Soc.,* **71,** 2125–2153.

Wielicki, B. A., B. R. Barkstrom, E. F. Harrison, R. B. Lee III, G. L. Smith and J. E. Cooper, 1996: Clouds and the Earth's radiant energy system (CERES): an Earth observing system experiment. *Bull. Amer. Meteor. Soc.,* **77,** 853-868.